Available online at www.sciencedirect.com

ScienceDirect

Energy Procedia 92 (2016) 153 – 159

Energy Procedia

6th International Conference on Silicon Photovoltaics, SiliconPV 2016

Simulation study of light-induced, current-induced degradation and recovery on PERC solar cells

Massimo Nicolai[a], Mauro Zanuccoli[a], Marco Galiazzo[b], Matteo Bertazzo[b], Enrico Sangiorgi[a], Claudio Fiegna[a]

[a]*Advanced Research Center on Electronic-Systems (ARCES), and DEI, University of Bologna, Via Venezia 52 Cesena (FC), 47521, Italy*
[b]*APPLIED MATERIALS ITALIA s.r.l., Olmi di San Biagio di Callalta (TV), 31408, Italy*

Abstract

The way to permanently recover the well-known Light-Induced Degradation (LID) which affects the p-type Cz-Si PERC solar cells represents one of the main challenges of photovoltaic research. In this work we have set up a numerical simulations flow which allows us to reproduce the experimental measured values of figures of merit (FOMs) of four different Cz-PERC solar cells lots subjected to a degradation and two regeneration processes. The recombination centres in bulk and the Boron-Oxygen complexes (B-O) are modeled by means of two trap levels tuned on the basis of experimental data. From simulations we confirm that the FOM degradation levels off after 16 hours and the regeneration process characterized by relatively long time process is preferred in terms of performance recovery. In addition, further cells with different passivation films are analyzed by adopting the same methodology.

Peer review by the scientific conference committee of SiliconPV 2016 under responsibility of PSE AG.

Keywords: Light-Induced Degradation (LID); c-Si; PERC solar cells; numerical simulations

1. Introduction

It is well known that boron doped p-type crystalline silicon solar cells exhibit Current-Induced Degradation (CID) and Light-Induced Degradation (LID) of cell performance [1]. This effect is generally ascribed to the activation of boron-oxygen (B-O) defects and is accompanied by a reduction in bulk minority-carrier lifetime. Such degradation is almost completely recoverable if a dedicated process, which causes B-O complex dissociation, is applied. Since PERC solar cells represent one of the most promising architecture [2], the study of CID/LID effects and the regeneration techniques in PERC solar cell has been theoretically and experimentally investigated by several groups [3-4].

Peer review by the scientific conference committee of SiliconPV 2016 under responsibility of PSE AG.
doi:10.1016/j.egypro.2016.07.014

In this work, starting from experimental Figures of Merit (FOMs) values and from the dark I-V characteristics of different samples post-recovery [5], we have set up a numerical simulation flow which allows us to calibrate the model to determine the degradation and the recovery conditions. In particular, as discussed in [6], B-O defects are taken into account by means of a properly tuned trap distribution. The analysis are performed on Cz-Si PERC solar cells from five different lots. The first four lots (Lot1 to Lot4) refer to a Al_2O_3 passivation film while the last considered lot (Lot5) features a SiO_x passivation. The cells are subjected to a CID and a subsequent regeneration process in different conditions and during these processes the FOMs of the cells are monitored.

The paper is organized as follows. In section 2, we describe the experimental characterization, by referring to a previous work [5]. In section 3, we illustrate the simulation methodology and the adopted physical models. In subsection 4.1, we discuss the experimental values of the five considered lots in terms of FOMs and saturation current densities J_{01} and J_{02} measured during the degradation process and after different regeneration processes. Finally, in section 4.2, the parameters adopted in the simulations which allow us to physically reproduce the performance trends are reported and analyzed.

2. Experimental methodology

The experimental characterization is performed on p-type Cz-Si PERC solar cells from 4 lots (Lot1 to Lot4), fabricated by using the same technology by different manufacturers. Process, geometrical and doping parameters have been not provided by suppliers. The degradation process, as discussed in detail in [5] consists in a CID (that is comparable to LID, by applying a current of 6A at temperature below than 45°C) during which the dark I-V parameters as well as the solar cell FOMs are monitored at intermediate time intervals up to 16h (Fig. 2 to Fig. 4). Before degradation process the I-V characteristic of all cells is measured. Moreover, for each lot two different regeneration processes (high temperature treatment together with high carrier injection and fast sample cooling [5]) are applied. These two processes are different in terms of duration (in the following paragraphs they are denoted by “short” regeneration and “long” regeneration) and are performed on the degraded cells and on the undegraded cells of the considered lots. The steps of regeneration are followed by a process of degradation in order to evaluate the recovery stability. Further details of the stability check of the recovery process are reported in [5].

It is worth noting that at the starting point the Lot1 has been already regenerated. As it will be discussed in Section 4, this explain why this lot is less sensitive to LID.

A further lot (Lot5), which differs from the others in terms of passivation film (SiO_x instead of Al_2O_3), has been subjected to same degradation process and monitored after 16 hours of degrade. The following regeneration process is applied at temperature of 230°C for 60 minutes.

In Fig. 1 a summary diagram of the discussed processes is reported.

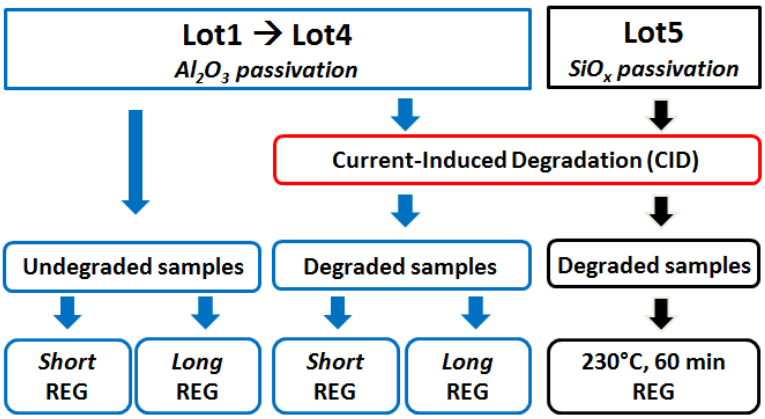

Fig. 1. Experimental methodology step diagram

3. Simulation methodology

Numerical simulations have been performed by using a TCAD device simulator [7]. We consider a simplified 1-D structure representing a p-type Cz-Si PERC solar cell. The cell is 180 µm-thick with substrate resistivity 1.5 Ωcm and exhibits a 75 Ω/sq homogeneous emitter. The PERC cell has an effective value of back surface recombination velocity of 60 cm/s. Simulations are carried out by considering the physical models parameters already successfully adopted in [8-20]. To account for the effective intrinsic carrier density, they include the band-gap narrowing model by Schenk [21]. For Auger recombination model the Altermatt's parameterization [12] is adopted as well as the Klaassen's mobility models [22, 23]. Moreover, Fermi-Dirac statistics are included. The optical generation rate profile refers to the standard AM1.5G spectrum (1000 W/cm^2) [24].

In order to reproduce the measured dark saturation current density J_{02} a tuning of an effective carrier lifetime (single level trapping, Shockley Reed Hall model) within a 1um-deep region which includes the emitter space charge region is carried out.

In the remainder of the cell (bulk region) we assume a two-level acceptor trap distribution to model the recombination losses. The first energy level position is centered in the midgap and allows us to fit the initial (non-degraded) solar cell FOMs. The second trap level is representative of the B-O complexes and its concentration value is tuned on the basis of each single process condition that has been applied to the cell. The second trap level is positioned at -0.2 eV from the midgap and the carrier capture cross sections are of $5 \cdot 10^{-17}$ cm^2. These parameters are comparable to those adopted in [6].

Starting from experimental data, the numerical simulation flow aimed at reproducing the measured values for each step of the degradation-regeneration process, can be summarized in three main steps. First, the measured dark I-V characteristic data is analyzed [9] and in order to fit the J_{01} and J_{02}, the carrier lifetime within the space charge region and the traps level concentration are properly set up. Then a fine tuning of FSRV values is performed in order to reproduce the experimental values of short circuit current density (J_{SC}). Lastly, a series resistance in post processing is considered in order to reproduce the measured values of fill factor and efficiency.

4. Results and discussion

4.1. Measured data

As it can be observed in Fig. 2, the first four lots show different initial conditions in terms of FOMs. Moreover, we note that the curve describing the FOM degradation levels off after 16h, which means that the B-O defects are almost activated.

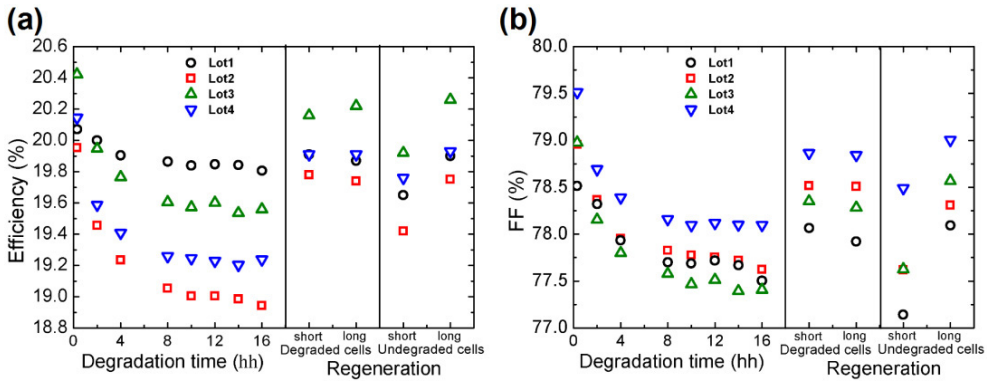

Fig. 2. Measured values of efficiency (a) and Fill Factor (FF) (b) for the first four lots in different conditions (degradation, "short" and "long" regeneration in case of degraded and undegraded cells).

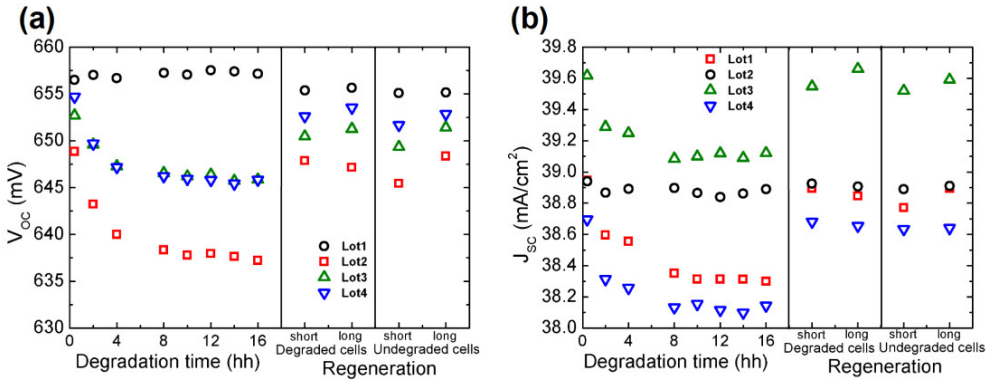

Fig. 3. Measured values of open circuit voltage (V_{OC}) (a) and short circuit current J_{SC} (b) for the first four lots in different conditions (degradation, "short" and "long" regeneration in case of degraded and undegraded cells).

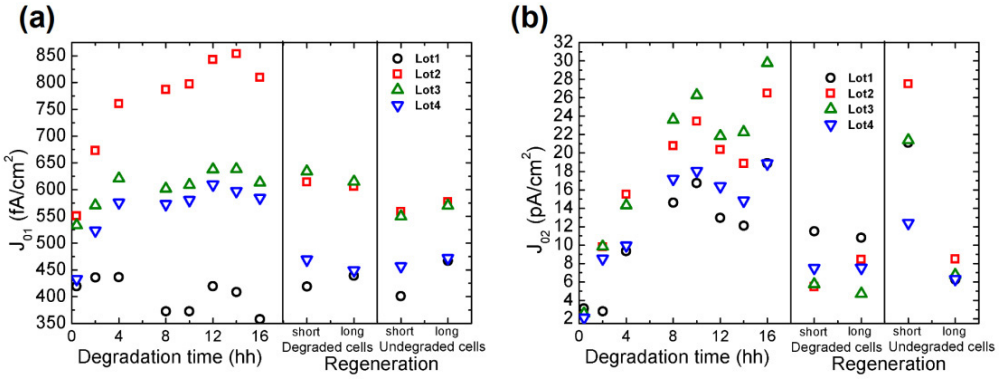

Fig. 4. Measured values of saturation current density J_{01} (a) and J_{02} (b) for the first four lots in different conditions (degradation, "short" and "long" regeneration in case of degraded and undegraded cells).

Table 1. Measured data of the Lot5 which differs from the others in terms of passivation film (SiO_x instead of Al_2O_3) for the considered conditions (start condition, degraded state and regenerated state)

Lot5	J_{SC} (mA/cm^2)	V_{OC} (mV)	FF (%)	Efficiency (%)	J_{01} (fA/cm^2)	J_{02} (pA/cm^2)
Starting point	39.45	661	79.16	20.66	400	6.7
Degraded (16 hours)	39.14	652	78.05	19.92	550	17.0
Regenerated (230°C, 60 min)	39.32	659	79.16	20.50	430	7.3

In case of degraded cells, the duration of the regeneration process ("short", "long") has no marked impact (Fig. 2 and Fig. 3) while in case of undegraded cells the "long" regeneration process leads to better FOMs recovery with respect to the "short" one. In detail, the effects of the process of stability check, aimed at evaluating the recovery stability [5], have a significant impact on the undegraded solar cells in case of "short" regeneration process. Due to stability check, FOMs recovery is not fully reached with respect to starting point. In terms of J_{01} (Fig. 4a) we observe that Lot1 exhibits the lowest values due to the fact that it has been previously regenerated and the effects of

the performed regeneration processes are negligible. Moreover, Lot3 and Lot4 show comparable values of J_{01} and no difference in terms of regeneration processes effectiveness is observable. However, Fig. 4b shows that, in case of undegraded cells, the "long" regeneration process leads to more marked J_{02} reduction.

The measured data of Lot5, which differently from the first four lots, features a SiO_x passivation film instead of Al_2O_3, are reported in Table 1. By comparing the initial conditions of Lot5 with the previous four lots we observe that efficiency and V_{OC} are subjected to a better recovery than others lots while J_{SC} and FF are substantially comparable with those of Lot3. Moreover, the J_{01} value confirms the advantages in terms of recombination losses observed for this lot. Regarding the regeneration process we observe a satisfactory recovery in terms of performance. In particular, respect to the first four lots, the grade of the recovery in terms of efficiency is slightly higher.

4.2. Simulation results

The consideration resulting from the analysis of the measured data are confirmed by simulation results (Fig. 5), which allow us to reproduce the experimental trends. In particular, the first level trap concentration values (reported in the caption of Fig. 5a) are consistent with the J_{01} values at the starting point and with the measured V_{OC} (Fig. 2a). From Fig. 5a, which illustrates the second level trap concentration versus process conditions, the saturation of the FOMs degradation curve and the B-O defects deactivation is not easily noticeable thanks to the regeneration process. Regarding the value of carrier lifetime within space charge region, simulations reveal that a regeneration process characterized by longer time is preferred in terms of performance recovery (Fig. 5b).

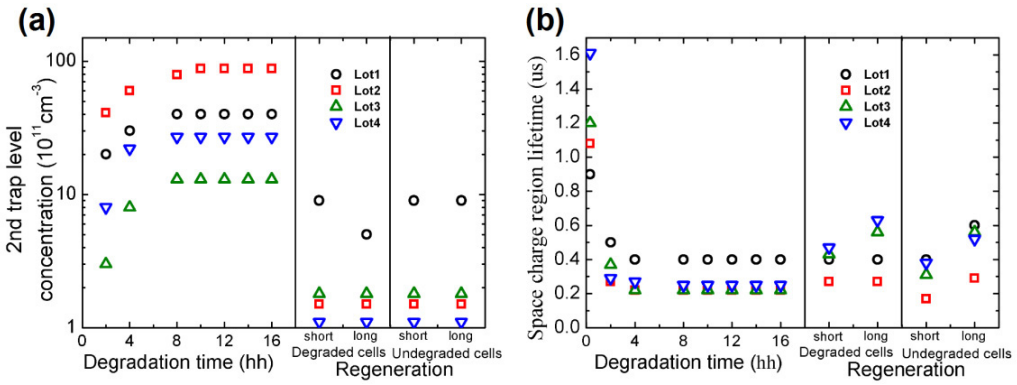

Fig. 5. (a) Values of 2nd trap level concentration for the first four lots in different conditions (degradation, "short" and "long" regeneration in case of degraded and undegraded cells) adopted in the simulations. The first level trap concentration values adopted in the simulations are $1.07 \cdot 10^{13}$ cm^{-3}, $1.65 \cdot 10^{13}$ cm^{-3}, $1.39 \cdot 10^{13}$ cm^{-3} and $1.22 \cdot 10^{13}$ cm^{-3} for the Lot1, Lot2, Lot3 and Lot4, respectively. (b) Values of the space charge region lifetime for the first four lots in different conditions (degradation, "short" and "long" regeneration in case of degraded and undegraded cells) adopted in the simulations.

Table 2. Values of the 1st and 2nd trap level concentration and of the space charge region (SCR) lifetime adopted in the simulations of the Lot 5 for the considered conditions (start condition, degraded state and regenerated state)

Lot 5	1st trap level concentration (10^{13} cm^{-3})	2nd trap level concentration (10^{11} cm^{-3})	SCR lifetime (μs)
Starting point	0.7	-	0.4
Degraded (16 hours)	0.7	15	0.1
Regenerated (230°C, 60 min)	0.7	1	0.3

Moreover, also the Lot5 is analyzed by means of the same simulation approach. The values of the trap levels concentration and the space charge region lifetime adopted in the simulation are reported in Table 2. The better

measured initial performance of this lot described in the previous subsection are confirmed by the 1st trap level concentration value which is smaller than those of all the previous lots (Fig.4a). In addition, the grade of the recovery is observable from the value of the 2nd trap level concentration. Although after degradation of 16 hours the 2nd trap level has relevant impact we can conclude that at the end of the recovery process (230°C for 60 min) the B-O complex are almost completely deactivated. The last consideration regards the space charge region lifetime. From the simulations results we note that after the regeneration process this lifetime is close to the starting point value and allow us to explain the behavior of the measured J_{02} value responsible to the FF variations.

Lastly, from simulation results it is worth noting that the series resistance contribution has not a relevant impact in terms of FOMs confirming the fundamental role of the trap density.

On the basis of our study, we can conclude that the effects of degradation and regeneration processes are well reproducible by considering B-O complexes activation and deactivation in the bulk region and in the space charge region. While the adoption of a proper trap distribution in the bulk is suitable to describe the behavior in terms of J_{01} and V_{OC}, the influence of the degradation-regeneration processes on FF and J_{02} could be reproduced only by tuning an equivalent carrier lifetime in the space charge region.

The PERC solar cells proposed in this work, which have been subjected to LID-CID and regeneration processes, exhibit efficiency recovery up to 98.9 %. The extent of the efficiency recovery is directly related to the duration of the process in accordance with [5]. However, in the case of lots previously regenerated (Lot1 in this work) the impact of LID-CID is less remarkable, leading to an efficiency recovery of 99.3 %.

5. Conclusions

In this work, we have analyzed the measured figures of merits (FOMs) and saturation current densities J_{01} and J_{02} of Cz-Si PERC solar cells from five different lots. The first four lots are characterized by a Al_2O_3 passivation film while the last lot features a SiO_x passivation. The cells are subjected to a Current-Induced Degradation process up to 16 hours where the FOMs are monitored at different intervals. Moreover, for each of the first four lot two different regeneration processes, which are different in terms of duration, are performed on the degraded cells and on the undegraded cells while in case of the SiO_x passivated lot the regeneration process is carried out at temperature of 230°C for 60 min only for degraded cells.

Starting from the experimental data, in order to reproduce the measured values for each step of the both degradation and regeneration processes, a numerical simulation flow is performed by using a TCAD standard simulator. In particular, with regards to the recombination losses in the bulk region we assume a two-level trap distribution. The first trap level allows us to fit the initial (non-degraded) solar cell FOMs while the second one is representative of the B-O complexes. The traps level concentration is properly tuned on the basis of each single process condition that has been applied to the cell in order to reproduce the measured data.

We observe that the curve describing the FOMs degradation levels off after 16h, which means that the B-O defects are almost activated, and in terms of recovery in the case of undegraded cells the regeneration process characterized by a longer time is preferable than the shorter one while in case of degraded cells, the duration of the regeneration process has no marked impact. The SiO_x passivated lot exhibits greater efficiency and V_{OC} than others lot and the J_{01} value confirms the advantages in terms of recombination losses. Regarding the regeneration process we observe that the grade of the recovery in terms of efficiency is slightly higher than previous lots.

On the basis of our simulation study, we can conclude that the adopted trap-model, in combination with a tuning of an equivalent carrier lifetime in the space charge region, correctly reproduce the influence of the degradation-regeneration processes on the FOMs of the presented solar cells.

References

[1] K.M. Broek, I.J. Bennett, M.J. Jansen, N.J.C.M. van der Borg and W. Eerenstein, Light and current induces degradation in p-type multi-crystalline cells and development of an inspection method and a stabilization method. Proc. 27th EU_PVSEC 2012;3167–3171.

[2] M. Zanuccoli, R. De Rose, P. Magnone, E. Sangiorgi and C. Fiegna, Performance analysis of rear point contact solar cells by three-dimensional numerical simulation. IEEE Trans. Electron. Devices 2012;59,1311-1319.

[3] A. Herguth, R. Horbelt, S. Wilking, R. Job and G. Hahn, Comparison of BO regeneration dynamics in PERC and Al-BSF solar cells. Energy Procedia 2015;77:75-82.

[4] S. Wilking, J. Engelhardt, S. Ebert, C. Beckh, A. Herguth, G. Hahn, High speed regeneration of BO-defects: improving long-term solar cell performance within seconds. Proc. 29th EU-PVSEC 2014;366-372.
[5] M. Martire, M. Bertazzo, M. Zamuner and M. Galiazzo, LID recovery tool for PERC solar cells. Proc. 31th EU-PVSEC 2015;879-883.
[6] T. Mchelidze and J. Weber, Direct detection of carrier traps in Si solar cells after light-induced degradation. Phys. Status Solidi RRL 2015;9:108-110.
[7] Sentaurus TCAD, Release J-2014.09, Synopsys, Zürich, Switzerland.
[8] A. Fell, K. R. McIntosh, P.P.. Altermatt, G.J. M. Janssen, R. Stangl, A. Ho-Baillie, H. Steinkemper, J. Greulich, M. Müller, B. Min, K. C. Fong, M. Hermle, I. G. Romijn and M. D. Abbott, Input parameters for the simulation of silicon solar cells in 2014. IEEE J. Photovoltaics 2015;5:1250-1263.
[9] R. De Rose, M. Zanuccoli, P. Magnone, E. Sangiorgi and C. Fiegna, Loss analysis of silicon solar cells by means of numerical device simulation. Proc. 14th ULIS 2013;205-208.
[10] M. Zanuccoli, P. Magnone, E. Sangiorgi and C. Fiegna, Analysis of the impact of geometrical and technological parameters on recombination losses in interdigitated back-contact solar cells. Sol. Energy 2015;116:37-44.
[11] G. Paternoster, M. Zanuccoli, P. Bellutti, L. Ferrario, F. Ficorella, C. Fiegna, P. Magnone, F. Mattedi and E. Sangiorgi, Fabrication, characterization and modeling of a silicon solar cell optimized for concentrated photovoltaic applications. Sol. Energy Mater. Sol. Cells 2015;134:407-416.
[12] P. Altermatt, Models for numerical device simulations of crystalline silicon solar cells-A review. J. Comput. Electron. 2011;10:314–330.
[13] M. Zanuccoli, J. Michallon, I. Semenihin, C. Fiegna, A. Kaminski-Cachopo, E. Sangiorgi and V. Vyurkov, Numerical simulation of vertical silicon nanowires based heterojunction solar cells. Energy Procedia 2013;38:216-222.
[14] R. De Rose, M. Zanuccoli, P. Magnone, E. Sangiorgi and C. Fiegna, Open issues for the numerical simulation of silicon solar cells. Proc. 12th ULIS 2011;84-87.
[15] P. Magnone, R. De Rose, D. Tonini, M. Frei, M. Zanuccoli, A. Belli, M. Galiazzo, E. Sangiorgi and C. Fiegna, Numerical simulation on the influence of via and rear emitters in MWT solar cells. IEEE J. Photovoltaics 2014;4:1032–1039.
[16] M. Nicolai, M. Zanuccoli, P. Magnone, D. Tonini, E. Sangiorgi and C. Fienga, Theoretical study of the impact of rear interface passivation on MWT solar cells. J. Comput. Electron. 2015;15:277-286.
[17] M. Zanuccoli, R. De Rose, P. Magnone, M. Frei, H.W. Guo, M. Agrawal, E. Sangiorgi and C. Fiegna, Numerical simulation and modeling of rear point contact solar cells. Proc. 37th IEEE PVSC 2011;1519–1523.
[18] R. De Rose, K. Van Wichelen, L. Tous, J. Das, F. Dross, C. Fiegna, M. Lanuzza, E. Sangiorgi, A.U. De Castro and M. Zanuccoli, Optimization of rear point contact geometry by means of 3-D numerical simulation. Energy Procedia 2012;27:197-202.
[19] P. Procel, V. Maccaronio, F. Crupi, G. Cocorullo, M. Zanuccoli, P. Magnone and C. Fiegna, Analysis of the impact of doping levels on performance of back contact – back junction solar cells. Energy Procedia 2014;55:128-132.
[20] I. Semenikhin, M. Zanuccoli, M. Benzi, V. Vyurkov, E. Sangiorgi and C. Fiegna, Computational efficient RCWA method for simulation of thin film solar cells", Opt. and Quant. Electron. 2012;44:149-154.
[21] A. Schenk, Finite-temperature full random-phase approximation model of band gap narrowing for silicon device simulation. J. of Appl. Phys. 1998;84:3684–3695.
[22] D. Klaassen, A unified mobility model for device simulation: I. Model equations and concentration dependence. Solid-State Electron. 1992;35:953–959.
[23] D. Klaassen, A unified mobility model for device simulation: II. Temperature dependence of carrier mobility and lifetime. Solid-State Electron. 1992;35:961–972.
[24] ASTM G159-98 Standard Tables for References Solar Spectral Irradiance at Air mass 1.5: Direct normal and hemispherical for a 37° tilted surface. Doi:10.1520/G0159-98.